XI International Conference on Computational Methods in Marine Engineering

Experimental investigation of iQFOiL lift and drag in a towing tank

Jamie Cook[1*] and Dr Joseph Banks[1]

[1] Faculty of Engineering and Physical Sciences, University of Southampton, Burgess Rd., Southampton SO16 7QF, UK
*jcmc1g21@soton.ac.uk

ABSTRACT

There has been limited towing tank testing for sailing hydrofoils producing both large forces and moments, due to the challenges this presents to dynamometry. In this paper, a windsurfing iQFOiL was tested in a towing tank using a new experimental rig to measure both lift and drag forces. Numerical predictions of the foil forces were estimated using XFLR5 to provide design loads for the dynamometry. The hydrofoil was tested up to speeds of $8\,\mathrm{ms}^{-1}$ and over a range of pitch angles, which affect the foil angle of attack. Repeat tests were conducted and the measurement uncertainty was calculated to assess the reliability of the developed dynamometry and test methods. It was found the equipment was capable of repeat readings within 0.5% when operating at realistic foiling speeds and could measure lift forces up to $1300\,N$. Additionally, the equipment had an average uncertainty of $6.43\,N$ and $2.19\,N$ for lift and drag measurements respectively. The interaction effects between the lift and drag forces measurements were assessed. Calibration and benchmarking showed a precision of 0.4% and a linear response up to $1300\,N$. Recommendations to improve the measurement accuracy are discussed and the suitability of the experiments for validation of numerical simulations are explored.

Keywords: Experimental hydrodynamics, Olympic sailing, hydrofoil, experimental uncertainty

1 Introduction

A hydrofoil is a control surface that creates lift through a pressure differential across its cross-section. At an angle of attack to the freestream, the fluid is accelerated over the top surface, resulting in a low pressure region relative to the slower moving fluid on the bottom surface (Bernoulli's principle). The pressure differential creates a resultant force on the control surface. Turnock (2008) details in-depth physics of hydrofoils and their application to sailing vessels.

A fully submerged foil sits with its whole lifting surface below the waterline. Therefore, as the lifting area is constant, more lift is produced as the inflow velocity increases. A vessel must then find a way of controlling the pitch or camber of the foil to change lift coefficient. This is usually done by adding a controllable flap on the rear of the foil or adjusting the rake of the whole foil. Furthermore, a fully submerged foil is less influenced by wave effects changing the lifting area, helping to reduce accelerations. The foil is also not subject to drag penalties caused by operation close to through the free surface, provided the control surface is acting in deep water (Poss, 2023). The control surface of a fully submerged foil will require a vertical strut to connect the foil to the board/hull. The most common arrangement is known as a $'T'$ foil, where the vertical is connected at the midpoint of the hydrofoil span. The centre of lift acts closely to the vertical strut and thus the moment where the top of the mast is fixed will be minimal.

Tandem foils, are longitudinally spaced hydrofoils, connected by a fuselage. The front, main foil provides the majority of the lifting force, with the rear foil used to increase the pitching stability of

the system. Two control surfaces allow a thinner hydrofoil section, increasing maximum achievable speed.

The iQFOiL, designed in 2018, is a foiling windsurfer, that made its Olympic debut in Marseille for the Paris 2024 games. The board is $2.2\,m$ long with a weight of $11.25\,kg$. When racing, the male class use an $8.0\,m^2$ sail whilst the females use a $7.3\,m^2$ sail.

The vertical strut is connected to the fuselage, on this fuselage a front and rear wing are bolted, shown in Figure 1. The rear foil is designed to generate down-force and hence a large pitching moment acts on the vertical mast as a result of the lift/downforce generated. This large moment presents a challenge to dynamometry when testing tandem foils compared to a conventional $'T'$ foil within a towing tank.

Figure 1: IQFOiL hydrofoil, showing the mast, fuselage, front and rear wing (Starboard, 2023).

Current iQFOiL athletes have expressed dissatisfaction with the quality consistency of the one design equipment, in particular, the foils. Initial CT scans of different foils have shown slight inconsistencies with the geometry of the foil, leading to performance differences. Due to the ever changing environmental conditions, it is impractical and time consuming to conduct on-water testing of equipment. Therefore, a method of testing hydrofoils in the more controlled environment of a towing tank is the first step towards quantification of differing foil characteristics.

There has been limited testing conducted on windsurfing specific hydrofoil kit within a towing tank. Research has been commonly aimed at model ships or small foiling dinghies such as the international foiling Moth. Whilst the foil configuration does vary, the principle of gathering data from a fully submerged foil is still highly relevant. Day et al. (2019) tested a moth hydrofoil in a towing tank, they found that simple models and predictions agreed with experimental data fairly well. Therefore, it is sensible to use simplified programs to predict forces when designing dynamometry for tow tank testing. Furthermore, simple models can reasonably predict the force changes for small geometry changes made to the foil, helping to define reasonable precision for the load sensors within the experimental rig. Likewise, using empirical formulas, a reasonable estimation of lift and drag forces can be predicted. Binns and Brandner (2008) released a conference paper discussing the effect of the free surface on performance of a moth rudder T-Foil. Binns tested the rudder in a towing tank, the rudder was fixed to a force balance previously designed by Binns and error analysis was carried out with the findings published (Binns, 2005). Their studies found as the foil got closer to the free surface there was a decrease in drag but also a decrease in lift. Furthermore, when sailing, iQFOiLs heel their equipment to windward to use the lift force generated by the foil as a contribution towards righting moment. One of Binns and Brandner (2008) conclusions was that from angles 0° to 30° there was no change in efficiency of the foil (also a conclusion of the CFD analysis by Ocaña-Blanco et al. (2017)). Therefore, to characterise the performance of the iQFOiL, applying heel won't be necessary and hence, reduces

the complexity of the rig. Kebbell and Binns (2022) used two Waszp foils in a tandem configuration to test an electronic ride height system. Their rig had a static frame connected to a carriage mounted on the bow of a boat. Kebbel and Binns then connected a dynamic frame that was free to heave and pitch. A load cell was connected between the static and dynamic frames to measure displacement and hence forces produced by the foil configuration. The system is allowed to heave on two slider rails, it was not mentioned how the moments may affect the heaving motion and hence lift measurement. The Waszp foils were attached to the frame using two 3D printed mounts that were clamped tight around the foil, although specific details were not given in the report. Likewise, Beaver and Zseleczky (2009) simply used two wooden supports around the foil secured with a saddle clamp. Beaver and Zselecky also used two gauges in a stacked arrangement to measure lift and drag forces. Underneath the force gauges were two metal plates with drilled location holes to adjust the pitch of the foil.

When designing an experimental rig, the accuracy of the dynamometry can limit the rigs ability to measure small changes in foil performance. It is expected that the iQFOiL system variation in performance will be small between slight geometrical or setup changes. The easiest way to benchmark a dynamometer's precision is by first calibrating the load cell, then hang known masses from the experimental rig and compare recorded force to applied force. Molland and Turnock (2002) designed dynamometry to measure propeller torque and found a repeatability of tests within 0.5% which was considered more than satisfactory. Furthermore, it was recommended that the calibration process should cover the loading and unloading of the system to check for hysteresis effects. When calibrating dynamometry, the elastic deformations of the equipment should be checked, to ensure that there is a linear response from the dynamometry across the expected loading conditions (Dubois, 1981). Provided the calibration of each force measuring component is satisfactory, the interference between the whole system can be investigated. It is suggested by Molland (1977) that first order interactions shall be determined by measuring the force recorded by a sensor when the system is loaded directly by perpendicular force. The interaction slope should then be determined via method of least squares linear regression.

Based on the above, the following aim was stated: Develop an experimental method to test tandem hydrofoils in the towing tank.

Objectives:

- Predict iQFOiL forces using a numerical method
- Design dynamometry that measures lift and drag forces with suitable repeatability
- Quantify precision of dynamometry
- Test iQFOiL over varying parameters

2 Methodology

2.1 XFLR5 force prediction

The hydrofoil wing cross sections were modelled in XFOIL, allowing XFLR5 wing analysis to give an estimate of forces. The wing section shapes were approximated as a NACA 2412 and the mast section shape was approximated as a NACA 0012. Using XFOIL direct analysis, the software considers the 2D sections and approximates the C_L and C_D for a sweep of AOA and Reynolds numbers.

The 3D iQFOiL setup was modelled in XFLR5 under the wing and plane design section. The following parameters could be changed at any point along the span to achieve the desired shape; chord, offset, dihedral angle and twist angle. The iQFOiL has a swept, dihedral shape, thus, to achieve an exact

replica was challenging. The mast was modelled in 3D with a span of 0.55 m so that only the submersed section was considered. It is recommended by the software to not include the fuselage in the CFD analysis due to poor expected results. After the foil had been modelled, the next step was to define the analysis. To replicate the experimental test matrix, a combination of fixed speed and varying AOA and vice versa was chosen. XFLR5 assumes inviscid flow and therefore does not calculate viscous effects. However, within the analysis window there is an option to include viscous effects. This is calculated for the 2D section in XFOIL and interpolated to the 3D plane in XFLR5, therefore viscous effects were included. For analysis of tandem foils, the horseshoe vortex method (VLM) was used, as the lifting line theory could only be applied to a singular wing.

At an inflow velocity of $8\,\mathrm{ms}^{-1}$ the CFD predicted 71.93 Newtons of drag and 1197.80 Newtons of lift, at a 4° pitch angle and a +1° rear wing chock. Although crude, an initial estimate of expected forces with the addition of safety factors aids the design of the experimental rig.

2.2 Experimental equipment

2.2.1 Force blocks

The University of Southampton provided six force blocks, three $100\,N$ capacity blocks that were orientated to measure horizontal forces (drag) and three $500\,N$ capacity blocks orientated to measure vertical forces (lift).

The force blocks have an LVDT clamped within its structure, with the probe pressed up against a face in the centre of the block, as seen by Figure 2. As force is applied the structure will deform, assuming a linearly elastic response the probe will either extend or retract and output a voltage change that is proportional to the force. The design of the block allows it to decouple the moment from the force. Figure 2a shows a pure moment applied to the block. The flexures of the block will be loaded in compression (shown by red arrows), provided the compression is below the critical buckling stress, the LVDT will record zero force. If a force was applied to the block as shown by the blue arrow, the flexures will deflect, the displacement will then be measured as a voltage by the LVDT.

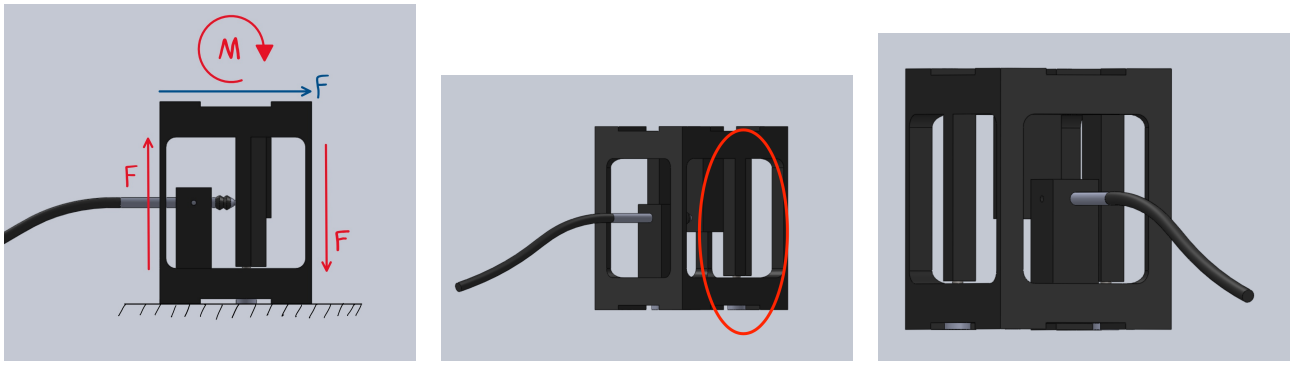

(a) (b) (c)

Figure 2: SOLIDWORKS images of a force block. The red arrows show the compression in the flexures as a result of an applied moment. The blue arrow shows a force applied to the block.

The tip of the LVDT has limited travel, thus, it is important to position the tip such that it does not run out of range before the maximum load is applied. Additionally, when the block is unloaded, the LVDT tip should sit at its mid-range of travel as to record zero voltage. Therefore, this was done after the rig had been fixed in the tow carriage. Furthermore, as shown by Figures 2b and 2c, the flexures are designed with a rectangular cross section, allowing the block to deform more in the desired degree of freedom. Thus, when clamped into the frame, care must be taken to orientate the blocks

to measure lift or drag forces. The blocks used were rated at $500\,N$ or $100\,N$, additional flexures can be seen on the block, shown by the red oval in Figure 2b. The flexure is only connected at one end of the block, with a pin located through the other end. When unloaded, there will be a gap between the pin and its hole. If the capacity of the block is exceeded, the block will deform, and the pin will press up against the side of the flexure, increasing the stiffness of the block as the additional flexures effectively become fixed at both ends (Figure 2b).

2.2.2 Experimental frame

The proposed experimental frame to house the force blocks and connection for the iQFOiL is shown in Figure 3. The lower frame is 'live', whereas the top frame is fixed to the carriage as per Figure 3b. The two frames are connected by the force blocks that measure force applied to the pitch plate, connected to the live frame. By separating the blocks in a rectangular arrangement, hence increasing the lever arm from the pitch plate to the force blocks, the buckling force on the flexures due to the large pitching moments from the foil is reduced.

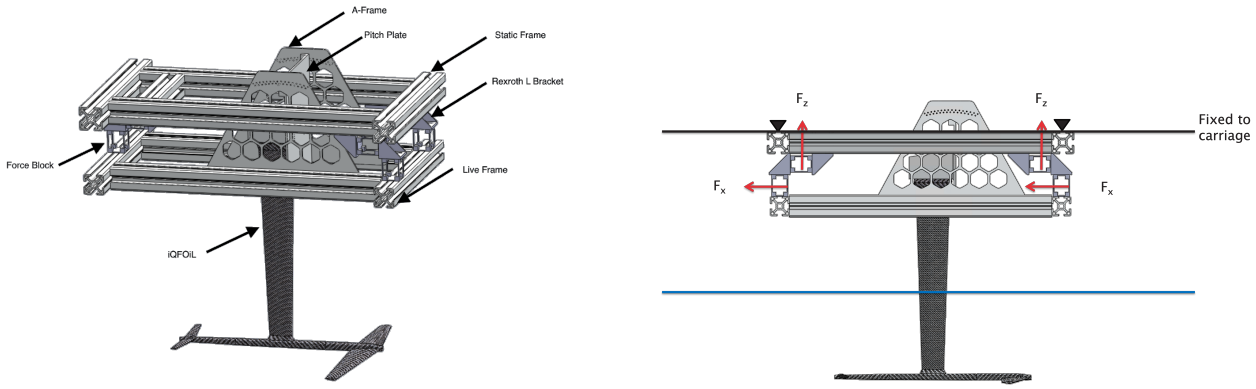

(a) (b)

Figure 3: SOLIDWORKS model of experimental frame, force blocks and foil.

The pitching plate is secured to an A-frame, with the pitch determined by a locator pin at the top. Hence, the angle can be adjusted in half degree increments. The iQFOiL was connected to the plate using a windsurf board 'Tuttle box', adhered to an aluminium plate. The tuttle box was then mechanically fastened to the pitching plate, allowing the variation of immersion (set at $0.55\,m$ from the fuselage). The longitudinal position of the A-frame along the live frame was positioned such that the lifting force was distributed equally between each force block.

2.2.3 Calibration and benchmarking

The midpoint of the LVDT's was found using the data acquisition box from the University of Southampton, by approximating the position so that the measured voltage was close to zero, this was fine-tuned using the zero screw on the RDP box. The gain of the channels were then adjusted to ensure the maximum output voltage did not exceed ± 6 volts when the maximum expected load was applied. The six outputs from the RDP box assigned to the three lift and three drag channels were plugged into the towing tank data acquisition system. Once the setup of wiring was completed, the drag was then calibrated by applying known masses to the pitch plate. A line was secured to the centre of the plate and threaded over a pulley bolted to the back of the static frame. Weights of $0\,N, 20\,N, 40\,N, 60\,N$ and $80\,N$ were applied to the calibration line. For each drag force block the weights were applied incrementally whilst acquiring the voltage difference. Whilst the blocks were calibrated individually,

as the applied weight is distributed between the three blocks, the total drag is an average of the three measured forces. For the lift, each force block was calibrated independently from the frame. The block was clamped in place, here known masses of $0\,N, 20\,N, 40\,N, 60\,N$ and $80\,N$ were used to calibrate the block. This approach meant that to calculate the total lift generated from the foil, a sum of the three lift measurements was used rather than an average.

As the lift force blocks were calibrated over a small weight range, the linearity of the dynamometry was tested over the full range of expected force. The rig was loaded up to $1317\,N$, 9.95% higher than the maximum expected force during the test matrix. Up to $1220\,N$ there was an average error of 0.4%, a linear response up to this point. However, at $1317\,N$ of applied force there was an error of 0.8%, Figure 4 highlights the start of a non-linear response at the highest applied force. It is important to note that as the force blocks are rated to $500\,N$, it is possible that due to improper placement of the LVDT, the probe may have reached the limit of its travel and produced an error. As the maximum expected force is under $1200\,N$ the system is assumed to have a linear response and hence the calibration coefficients hold, when unloading the equipment, hysteresis effects were also checked and determined satisfactory.

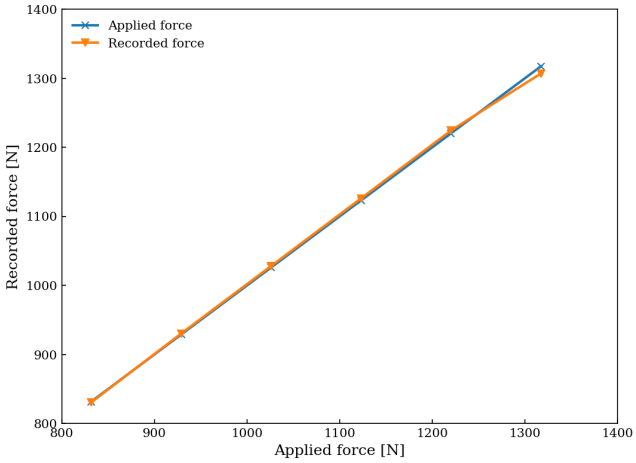

Figure 4: Applied force against recorded force for lift applications over expected range.

The last step of the calibration was to consider the interference between the lift and drag forces due to the bending of the rig. When large lift forces were applied, the rig can be modelled as a beam, clamped at both ends. The curvature of the Rexroth frame causes a voltage change in the drag channels known as parasitic drag. A paper on the design of dynamometry by Molland (1977) recommends finding the parasitic drag as a function of lift, and the parasitic lift as a function of drag, better known as an interference matrix. This test was again conducted in the model preparation area when the rig was positioned on trestles. A lift force of up to $1250\,N$ was applied to the frame whilst the drag voltages were acquired, using the known calibration coefficient for each drag block, the parasitic drag could be calculated as a function of applied lift. The parasitic lift was investigated, however, was considered negligible due to the small drag forces expected. This reduces the interference matrix down to the first order response shown by equation 1, determined via the graphical relationship between lift and parasitic drag.

$$\text{Parasitic drag} = 0.02 \times L \tag{1}$$

Where L is the measured total lift during a test run. A large proportion of the parasitic drag was measured by the rear force block. This is due to the centre of lift being positioned towards the front of the rig, hence the lever arm and bending moment is far higher for the aft force block. Whilst the force block should not be affected by large moments, if the structure in which it is bolted to deforms, the measurements will be affected. As the drag is positive, the parasitic drag must be subtracted from the total drag measured by each test run.

3 Results and discussion

3.1 Post processing

For each run, the towing tank data acquisition stored each data channel in a CSV file. Each file contained voltage data from each force block, carriage speed and time. Hence, the lift and drag could be calculated in newtons and plotted against time. A python script was used to remove noise from the data and a function automaticity windowed each run to determine the quasi-steady state force values. Using the windowed data, the type A uncertainty was calculated and combined with the type B uncertainties for combined error bars. An example of a run conducted at $8\,ms^{-1}$ is shown by Figure 5.

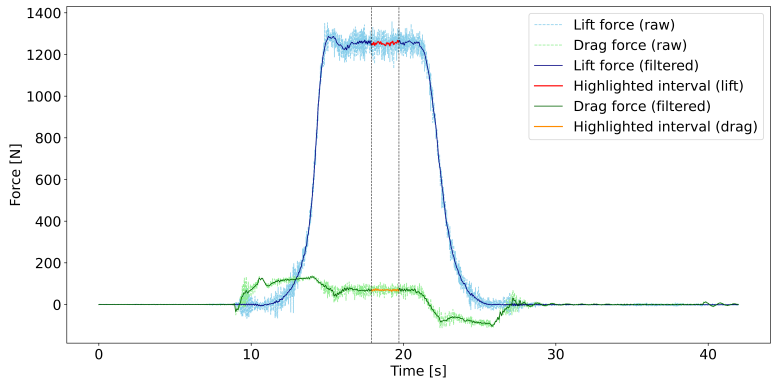

Figure 5: Example of post processing to obtain average lift and drag values from each run. The figure shows a run at $8\,ms^{-1}$, pitch of $+2°$ and rear wing angle of $+1°$.

3.2 Pitch sweep

The equipment was used to conduct a sweep of foil pitch from $-4°$ to $2°$, at a carriage speed of $8\,ms^{-1}$ and rear wing angle of $+1°$. During testing, the plate's angle was measured using an inclinometer, the error was found to be within $\pm 0.10°$ of the stated value, thus considered small. Moreover, when the rig was set at the $0°$ setting on the pitch plate, the bottom of the bonded Tuttle box was measured as $89.90°$ with respect to the vertical plane. Therefore, the test was conducted with the assumption of the board, at the section where the foil connects, being parallel to the water at $0°$ pitch. The tandem system is raked aft from the board, hence, the negative lift reading at $0°$ shown in Figure 6.

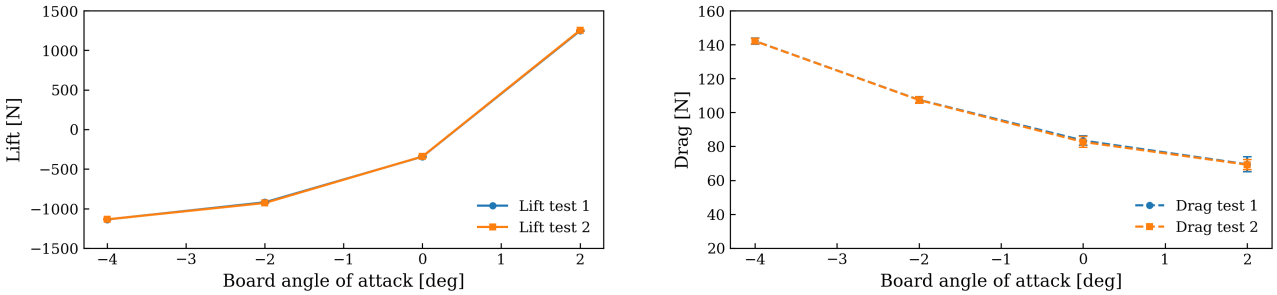

(a) Lift

(b) Drag

Figure 6: Measured lift and drag for varying AOA of system using Pitch plate with repeat reading ($v = 8ms^{-1}$, $Rear\,wing\,chock = 1°$).

Figure 6 shows a close agreement between repeat tests. The percentage difference is 0.41% for lift

and 0.43% for drag. Likewise, the average uncertainty value, U, was 6.43 N for lift and 2.19 N for drag. The pitch sweep shows a non-linear increase in lift, this is likely attributed to deformations in the experimental frame, fuselage and the hydrofoils under load. Furthermore, Figure 6b shows a non-linear decrease in drag throughout the tested range, it is expected that curve will reach a minima and thus, increase as board angle increases. For a cambered hydrofoil, the lift-induced drag will cause an offset of the minimum drag away from 0° AoA, although in this case the exact hydrofoil pitch angle is not known.

3.3 Tear drag

It is uncommon for computational simulations to model the mast. Therefore, the mast was towed through the water at various speeds with one repeat reading. The recorded drag can then be deducted from the drag from the previous tests for comparative purposes with CFD.

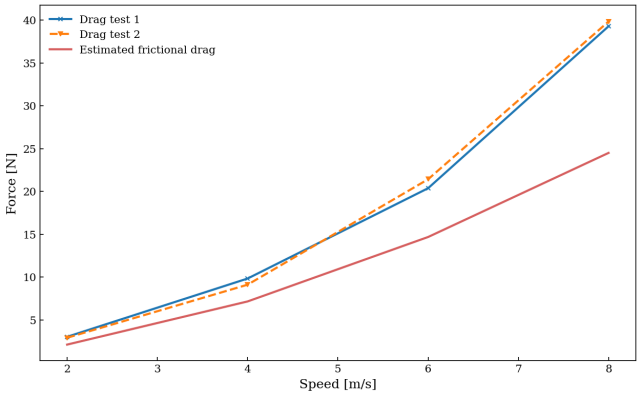

Figure 7: mast drag at increasing carriage speeds, conducted at a pitch of 0°.

The end of the mast has a lower male section, that is exposed when the fuselage is removed. In Figure 7, an estimation of the frictional drag is plotted using the ITTC57 empirical method and follows a similar trend to the measured drag. The difference from the frictional drag can be attributed to form and wave drag.

XFLR5 was used to predict the likely forces acting on the equipment during the test matrix. It was found that there was mean percentage difference of 43% and 45% between the experimental and XFLR5 lift and drag respectively across the same pitch sweep shown in Figure 6. At the highest recorded experimental lift force, XFLR5 under predicted by 394.8 newtons. Therefore, a safety factor of 1.5 would be sufficient to design the dynamometry.

4 Conclusions

The methodology and calibration procedure was outlined for this new experimental equipment. The results shown indicate that the repeatability of under 0.5% increases confidence in results. Whilst the benchmarking conducted shows the high precision and linearity of the dynamometry within the expected range. Furthermore, the effect of dynamometry deformation should be further investigated, continuing the work conducted in the interaction matrix.

The future work for this equipment will involve a calibration method within the carriage, ideally over the full range of expected forces. The foil will then be tested at a leeway angle, in regular waves and foil setup changes.

ACKNOWLEDGEMENTS

Conducted as part of the undergraduate programme at the University of Southampton, this project benefited from the generous support of British Sailing and Sam Sills, who provided the iQFOiL equipment.

References

B. Beaver and J. Zseleczky. Full scale measurements on a hydrofoil international moth. In *The 19th Chesapeake Sailing Yacht Symposium, March, Chesapeake*, 3 2009. URL 10.5957/CSYS-2009-013.

J. Binns. *Extreme Motions of Modern Sailing yachts - Quantifying Re-righting*. PhD thesis, 3 2005. National Centre for Maritime Engineering and Hydrodynamics, Australian Maritime College.

J. R. Binns and P. Brandner. The effect of heel angle and free-surface proximity on the performance and strut wake of a moth sailing dinghy rudder t-foil. In *The 3rd High Performance Yacht Design Conference, Auckland, NZ*, pages 121–129, 2008.

S. Day, M. Cocard, and M. Troll. Experimental measurement and simplified prediction of t-foil performance for monohull dinghies. In *The 23rd Chesapeake sailing yacht synposium, Chesapeake*, 2019.

M. Dubois. Six-component strain-gage balances for large wind tunnels. *Experimental Mechanics*, 21:401–407, 1981. ISSN 1741-2765. doi: 10.1007/BF02327141. URL https://doi.org/10.1007/BF02327141.

S. Kebbell and J. Binns. Development of a full scale moth hydrofoil control system test rig. *The 9th Conference on Computational Methods in Marine Engineering (Marine 2021)*, 1, 1 2022. URL 10.2218/marine2021.6863.

A. F. Molland. The design, construction & calibration of a five-component strain gauge and tunnel dynamometer. 1977. URL https://api.semanticscholar.org/CorpusID:108179103.

A. F. Molland and S. R. Turnock. A propeller thrust and torque dynamometer for wind tunnel models. *Strain*, 38:3–10, 2002. doi: https://doi.org/10.1046/j.0039-2103.2002.00001.x. URL https://onlinelibrary.wiley.com/doi/abs/10.1046/j.0039-2103.2002.00001.x.

D. Ocaña-Blanco, I. Castañeda-Sabadell, and A. Souto-Iglesias. Cfd and potential flow assessment of the hydrodynamics of a kitefoil. *Ocean Engineering*, 146:388–400, 12 2017. ISSN 00298018. URL 10.1016/j.oceaneng.2017.09.040.

J. Poss. Design and construction of a fully submerged hydrofoil drone boat. Master's thesis, 2023. URL https://hdl.handle.net/1721.1/152137. Bachelor thesis, Massachusetts Institute of Technology. Department of Mechanical Engineering.

Starboard. Official iqfoil senior equipment. ONLINE, 12 2023. URL https://iqfoil.star-board.com/equipment/iqfoil-class/. Acsessed 10/12/2023.

S. R. Turnock. Investigation of the effects of hydrofoil set-up on the performance of an international moth dinghy using a dynamic vpp, 2008. URL https://www.researchgate.net/publication/277761615.